Diversity of Human Insulin-like Growth Factor (IGF) Binding Protein-2 Fragments in Plasma: Primary Structure, IGF-Binding Properties, and Disulfide Bonding Pattern†

Silke Mark,‡ Bernd Kübler,§ Stefan Höning,|| Sandra Oesterreicher,§ Harald John,‡ Thomas Braulke,§ Wolf-Georg Forssmann,‡ and Ludger Ständker*,‡

IPF PharmaCeuticals GmbH, Feodor-Lynen-Strasse 31, D-30625 Hannover, Germany, Children's Hospital, University of Hamburg, D-20246 Hamburg, Germany, and Institute for Biochemistry II, University of Göttingen, D-37073 Göttingen, Germany

Received October 7, 2004; Revised Manuscript Received December 23, 2004

ABSTRACT: The insulin-like growth factor binding proteins (IGFBPs) play a major role in the regulation of the effects and the bioavailability of the insulin-like growth factors (IGFs). IGFs are released from IGFBP−IGF complexes by proteolysis of IGFBPs generating fragments with reduced ligand-binding properties. To identify naturally occurring fragments of IGFBP-2, a peptide library generated from human hemofiltrate was immunologically screened. Purification of immunoreactive IGFBP-2 fragments was performed by consecutive chromatographic steps. A total of 18 different IGFBP-2 fragments was isolated and characterized. The peptides exhibited different N-terminal amino acid residues that were located in the variable midregion of IGFBP-2. Four major cleavage sites were determined to be between Tyr103 and Gly104, Leu152 and Ala153, Arg156 and Glu157, and Gln165 and Met166. The resulting fragments were further processed by amino and/or carboxy peptidases and comprised 37−185 amino acid residues. Ligand blotting, solution binding assays, and BIAcore analyses revealed that all tested fragments retained low IGF-binding capacity. The most abundant fragment IGFBP-2 (167−279) showed 10% of IGF-II binding compared to recombinant human (rh)IGFBP-2. Furthermore, the disulfide bonding pattern of the C-terminal domain of rhIGFBP-2 was defined, indicating linkages between cysteine residues 191−225, 236−247, and 249−270. This study provides the most comprehensive molecular characterization of human IGFBP-2 fragments formed *in vivo*, exhibiting both residual IGF-binding capacities and the integrin-binding sequence.

The six insulin-like growth factor binding proteins (IGFBP-1−6)[1] are key components of the insulin-like growth factor (IGF) system contributing to the growth and differentiation of many cell types (*1*, *2*). They modulate cell and tissue function by regulating IGF bioavailability, i.e., inhibition of IGF action by sequestration of the growth factor (*3*), but also IGF-promoting and IGF-independent activities have been described (*4*−*8*). In plasma, ternary complexes of IGFBP-3 or IGFBP-5, the acid-labile subunit, and one molecule of IGF-I or IGF-II function as a reservoir, prolonging the half-lives and preventing glomerular filtration of IGFs. The less abundant binary IGFBP−IGF complexes are proposed to leave the circulation and localize to specific tissue compartments (*9*).

IGFBP-2 is the second most abundant IGFBP in the circulation known to form binary complexes with IGF. The nonglycosylated 31-kDa protein comprises 289 amino acids and consists of a central protease-sensitive and variable region encompassed by two globular and conserved cysteine-rich N- and C-terminal domains (amino acid residues 1−100 and 166−289, respectively). IGFBP-2 binds preferentially to IGF-II compared to IGF-I (*10*), and both terminal domains were recently shown to bear residual IGF-binding properties (*11*−*15*). Additionally, the C-terminal domain contains a proteoglycan-binding as well as an Arg-Gly-Asp (RGD) integrin-binding site, allowing the binding of IGFBP-2 to the cell surface (*6*, *16*).

After IGFBP-2 binding to the cell surface, its IGF affinity is decreased (*17*). Also proteolysis of IGFBPs generates IGFBP fragments with reduced IGF affinities, thus favoring the dissociation of the IGFs and enabling them to bind to cellular IGF receptors (*7*). Several IGFBP-specific proteases belonging to different classes of neutral serine, disintegrin, and matrix metalloproteases, as well as acid-activated cathepsins, have been described and characterized so far (*18*−*24*).

The goal of our study was to give a comprehensive description of IGFBP-2 fragments occurring in the human

† Supported by the Deutsche Forschungsgemeinschaft (Graduiertenkolleg 336; to S.O.).

* To whom correspondence should be addressed: IPF PharmaCeuticals GmbH, Feodor-Lynen-Strasse 31, D-30625 Hannover, Germany. Phone: +49-511-5466-329. Fax: +49-511-5466-132. E-mail: l.staendker@ipf-pharmaceuticals.de.

‡ IPF PharmaCeuticals GmbH.

§ University of Hamburg.

|| University of Göttingen.

[1] Abbreviations: ESI−MS, electrospray ionization−mass spectrometry; HF, hemofiltrate; MALDI−MS, matrix-assisted laser desorption ionization−mass spectrometry; IGF, insulin-like growth factor; IGFBP, insulin-like growth factor binding protein; rh, recombinant human; RP, reverse phase; SDS−PAGE, sodium dodecyl sulfate−polyacrylamide gel electrophoresis; CRF, chronic renal failure; CZE, capillary zone electrophoresis.

10.1021/bi0478401 CCC: $30.25
Published on Web 02/08/2005

circulation. Information about their structure and proteolytic cleavage sites and potential conclusions about the involved proteases and resulting functional consequences were expected.

Here, we present the isolation of 18 distinct fragments of IGFBP-2 from human hemofiltrate (HF) comprising the variable central and/or C-terminal domain. The major occurring IGFBP-2 fragments were purified and analyzed concerning their primary structure and IGF-binding abilities. The disulfide bonding pattern of the C-terminal domain was determined.

MATERIALS AND METHODS

Preparation of a Peptide Library from Human HF. Peptides of human blood ultrafiltrate (HF) were prepared as described recently (*15*, *25*). The peptides were extracted from 10 000 L of HF obtained from a local nephrological center and collected from 40 adult patients with chronic renal disease. Immediately after blood filtration using ultrafilters with a specified cutoff of 30 kDa, the filtrate was routinely chilled to 4 °C and adjusted to pH 3 to prevent bacterial growth and proteolysis. After dilution with deionized water to a conductivity of <8 mS/cm, batches of 800−1000 L of HF were adjusted to pH 2.7 by hydrochloric acid and applied to a strong cation exchanger [2 L Fractogel TSK SP 650-(M), Merck, Darmstadt, Germany]. Subsequently, the peptides were batch-eluted with 10 L of 0.5 M ammonium acetate at pH 7.0. To eliminate remaining amounts of plasma albumin in the concentrated HF, an additional ultrafiltration step was carried out with pooled batch eluates corresponding to 10 000 L equivalents of HF. This ultrafiltration was performed using a sartocon-mini ultrafilter (0.1 m^2, ps-membrane, Sartorius, Göttingen, Germany) with a specified cutoff of 30 kDa. Filtration was driven by a transmembranous pressure gradient of 1 bar at a temperature of 5 °C and a flow rate of 5−6 L/h. For the first separation step, the ultrafiltrate was diluted with deionized water to a conductivity of 6.7 mS/cm, adjusted to pH 2.7 with HCl, and applied to a second 10 L Fractogel cation-exchange column. The column was washed with 0.01 M HCl until the conductivity was below 1 mS/cm. Stepwise batch elution of the bound peptides was performed using the following eight buffers: (1) 0.1 M citric acid at pH 3.6, (2) 0.1 M acetic acid and 0.1 M sodium acetate at pH 4.5, (3) 0.1 M malic acid at pH 5.0, (4) 0.1 M succinic acid at pH 5.6, (5) 0.1 M NaH_2PO_4 at pH 6.6, (6) 0.1 M Na_2HPO_4 at pH 7.4, (7) 0.1 M ammonium carbonate at pH 9.0, and (8) water at pH 7.0 as a desalting step. The resulting pH-pool eluates (15−25 L) were collected, acidified to pH 2−3, and immediately subjected to a second separation step using reverse-phase (RP) chromatography. Each eluate was loaded onto a Source RPC column [100 × 125 mm inside diameter (id), 300 nm, 15 μm, Pharmacia, Freiburg, Germany] and washed with two column volumes of solvent A (10 mM HCl). The separation was performed at a flow rate of 200 mL/min using a 8 L gradient from 100% A to 60% B [80% acetonitrile (v/v) and 10 mM HCl]. Fractions of 200 mL were collected, and the absorbance at 280 nm was monitored. Aliquots of these peptide fractions were lyophilized and tested for IGFBP-2 immunoreactivity as described below.

Isolation of Immunoreactive IGFBP-2 Fragments. Western immunoblotting was performed as described previously (*15*, *26*). In brief, aliquots of the high-performance liquid chromatography (HPLC) fractions corresponding to 200 mL equivalents of HF were lyophilized, reconstituted in non-reducing sample buffer, and separated by TRICINE sodium dodecyl sulfate−polyacrylamide gel electrophoresis (SDS−PAGE). The separated peptides were transferred to a hydrophilic poly(vinylidene difluoride) (PVDF) membrane, blocked with 5% aqueous powdered skimmed milk, and incubated with rabbit recombinant human (rh)IGFBP-2 antiserum (Upstate Biotechnology, Lake Placid, NY) diluted to 1:1000. After incubation with goat anti-rabbit IgG coupled to alkaline phosphatase (Sigma, Deisenhofen, Germany) or goat anti-rabbit IgG coupled to horseradish peroxidase (Dianova, Hamburg, Germany; 1:10 000), reactive bands were visualized using a bromochloroindolyl phosphate/nitro blue tetrazolium substrate system as recommended by the manufacturer (Sigma) or detected by the SuperSignal enhanced chemiluminescence (ECL) detection system (Pierce Chemicals, Rockford, IL). Immunoreactive fractions were additionally analyzed by matrix-assisted laser desorption ionization−mass spectrometry (MALDI−MS).

Purification of naturally occurring IGFBP-2 fragments from the HF peptide library was achieved by consecutive chromatographic steps of immunoreactive fractions as exemplarily described for the 20-kDa fragments. For isolation, six additional semipreparative and analytical RP and cation-exchange chromatographic steps were performed. As solvents in RP chromatography, 0.1% trifluoroacetic acid (TFA) (solvent A) and 80% (v/v) acetonitrile containing 0.1% TFA (solvent B) were used. For cation-exchange chromatography, 50 mM NaH_2PO_4 at pH 3.0 (buffer A) and 50 mM NaH_2PO_4 containing 1.5 M NaCl at pH 3.0 (buffer B) were applied. (Step 1) The immunoreactive fractions from pH-pool eluate 5 were applied to a Source Fineline 15 RPC column (151 × 100 mm id, 34 nm, 15 μm, Pharmacia, Freiburg, Germany) and eluted at a flow rate of 150 mL/min with a linear gradient from 5 to 50% of solvent B over the course of 53.3 min. (Step 2) For further purification, a Bakerbond RP-C18 cartridge (300 × 47 mm id, 15−20 μm, Waters, Milford, MA) under a flow rate of 30 mL/min and using a linear gradient from 10 to 70% of solvent B in the course of 61.7 min was applied. (Step 3) Further chromatography was carried out on a cation-exchange column (Biotek Pepkat; 150 × 20 mm id, 100 nm, 7 μm, Biotek, Östringen, Germany) under a flow rate of 4.2 mL/min and using a linear gradient from 20 to 90% of buffer B over a course of 70 min. (Step 4) The isolation was continued by use of a Vydac RP-C18 column (250 × 20 mm id, 30 nm, 10 μm, Vydac, Hesparia, CA) under a flow rate of 7 mL/min. A linear gradient from 25 to 55% of solvent B over a course of 60 min was applied. (Step 5) The purification was continued using a Jupiter RP-C5 column (250 × 10 nm id, 30 nm, 5 μm, Phenomenex, Aschaffenburg, Germany) under a flow rate of 1.8 mL/min and using a linear gradient from 33 to 48% of solvent B over a course of 45 min. (Step 6) The final isolation step was performed on a Jupiter RP-C4 column (250 × 4.6 mm id, 30 nm, 5 μm, Phenomenex) under a flow rate of 0.7 mL/min and using a linear gradient from 33 to 48% of solvent B over a course of 45 min.

Peptide Analysis. The purity of isolated peptides was investigated by capillary zone electrophoresis (CZE) using a P/ACE system 2000 (Beckman, San Ramon, CA) supported

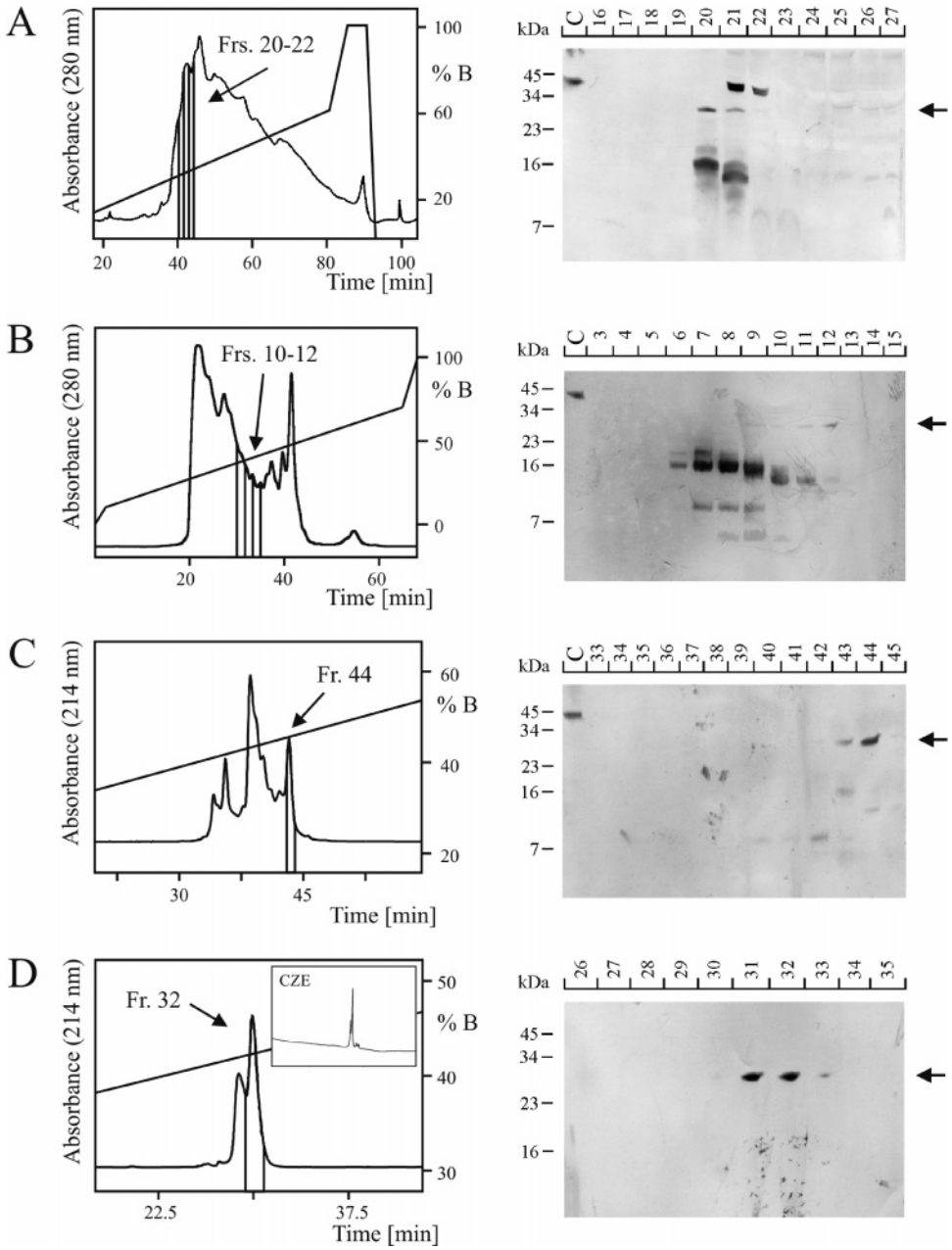

FIGURE 1: Purification of 20-kDa IGFBP-2 fragments from human HF. (A) Human HF peptide library was screened by Western blotting using polyclonal anti-IGFBP-2 antibodies. The pH-pool fraction 5 (*15*) known to contain the majority of immunoreactive IGFBP-2 material was separated by RP-HPLC (left panel). Each of the resulting 46 fractions was tested by IGFBP-2 Western blotting (right panel). All IGFBP-2 immunoreactive material was found in fractions 20−22 shown as bars (left panel). The purification of individual IGFBP-2 fragments combining consecutive chromatographic steps and Western immunoblotting of the resulting fractions is exemplarily shown for 20-kDa IGFBP-2 fragments using chromatographic steps described in the Materials and Methods, e.g., (step 2) preparative RP-C18 chromatography (15−20 μm) (B), (step 4) analytical RP-C18 chromatography (10 μm) (C), and (step 6) analytical RP-C4 chromatography (5 μm) (D). The immunoreactive band with an apparent molecular mass of 27 kDa is indicated by an arrow. Finally, the purity of the isolated fragments was determined by CZE (inset of D). The CZE of this purfication shows two main peaks, which were not separated by the chromatographic techniques used.

by the System Gold software. A fused silica uncoated capillary column (50 cm × 75 μm, Polymicro Technologies, Phoenix, AZ) was used with a 0.1 M sodium phosphate buffer containing 0.02% (w/v) (hydroxypropyl)methylcellulose at pH 2.5 and 25 °C. The separation was carried out with a constant current of 80 μA, and the peptides were detected at 200 nm using an integrated UV detector. Mass determination of the purified peptides was carried out on a Sciex API III quadrupole mass spectrometer (Sciex, Perkin−Elmer, Langen, Germany) with an electrospray ionization interface. Mass analysis of fractions was performed with a LaserTec RBT II MALDI−MS (Applied Biosystems, Darmstadt, Germany) as described previously (*26*). Peptides were sequenced on an 473 A gas-phase sequencer (Applied Biosystems) by Edman degradation with on-line detection of phenylthiohydantoin amino acids using the standard protocol recommended by the manufacturer. To analyze the disulfide bonding pattern of the C-terminal IGFBP-2 domain, proteolytic cleavage of purified native peptides was performed by the endoprotease chymotrypsin (sequencing grade from Roche Diagnostics, Mannheim, Germany). For digestion, the peptide was incubated using a peptide/enzyme ratio

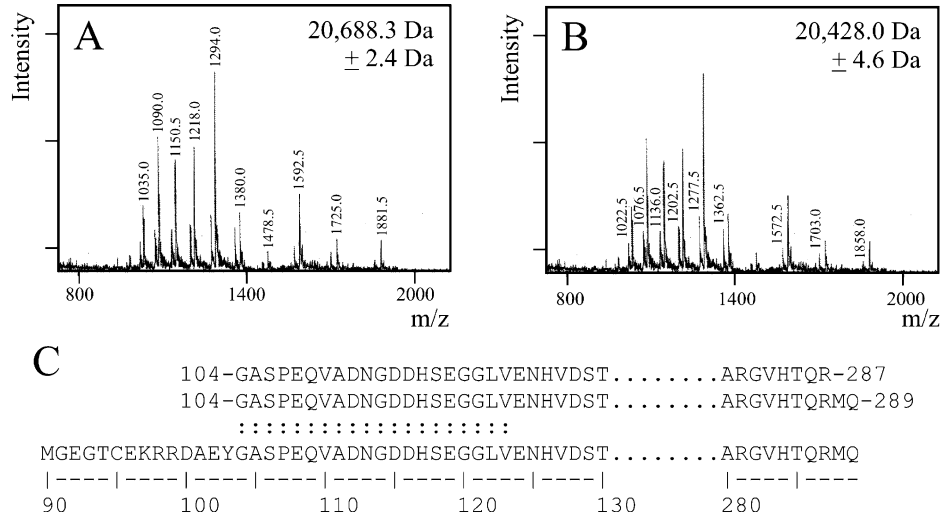

FIGURE 2: MS analysis and sequence alignment of 20 kDa IGFBP-2 fragments. The purified 20 kDa IGFBP-2 fragments were analyzed by ESI−MS (A and B) yielding molecular masses of 20 688.3 ± 2 and 20 428.0 ± 5 Da, respectively. N-terminal sequence analysis resulted in a common sequence GASPEQVADNGDDHSEGGLV for both fragments. (C) Alignment with the sequence of human IGFBP-2 and a comparison to predicted molecular masses identified two IGFBP-2 fragments comprising the amino acid residues 104−287 and 104−289 both starting with Gly104 but varying in their C termini.

of 1:100 (w/w) for 8 h at 25 °C in 0.1 M Tris-HCl at pH 7.8 as recommended by the manufacturer. The resulting fragments were separated by analytical RP-C18 HPLC and characterized by ESI−MS, MALDI−MS, and sequence analysis.

IGF-Binding Analysis. rhIGF-I was purchased from PeproTech (London, U.K.), and biotinylated IGF-II and intact rhIGFBP-2 were purchased from GroPep (Adelaide, Australia). Ligand blotting using [^{125}I]IGF-I and biotinylated IGF-II was performed as described previously (*27*−*29*). [^{125}I]IGF-I saturation studies were carried out as described previously (*28*). The equilibrium rate constants (K_d values) were determined by nonlinear curve fitting using the GraphPad Prism software version 3.0. Real-time binding of intact and IGFBP-2 fragments to IGF-II was analyzed by surface plasmon resonance (SPR) using a BIAcore 3000 (BIAcore AB, Uppsala, Sweden). The on rate (k_a) and off rate (k_d) as well as the equilibrium rate constants (K_d values) were calculated with the BIAcore evaluation software 3.1 assuming a simple 1:1 interaction between IGF-II and IGFBP-2.

RESULTS

Identification, Purification, and Primary Structure Analysis of IGFBP-2 Fragments in HF. A peptide library was generated from 10 000 L of human HF by cation-exchange chromatography (not shown) followed by preparative RP chromatography of the resulting batch eluates. The RP chromatography fractions were examined for IGFBP-2 immunoreactive peptides using a polyclonal antiserum proofed to recognize both the N- and C-terminal domain of IGFBP-2 (data not shown). Fractions eluting from the cation-exchanger eluate 5 (see ref *15* and Figure 1A) contained the intact 31-kDa IGFBP-2 molecule and various IGFBP-2 fragments with apparent molecular masses of 27, 18, 16, 15, 14, 10, and 4 kDa, as visualized by Western blotting (parts A and B of Figure 1). All IGFBP-2 fragments were subsequently purified by a combination of various RP and cation-exchange chromatographic steps to maximal homogeneity.

Three further steps of the purification procedure of the apparent 27-kDa IGFBP-2 fragment (parts B−D of Figure 1) and its subsequent identification are shown exemplarily for all fragments. Capillary zone electrophoresis was used to evaluate the final purity of the preparation (inset in Figure 1D) yielding two main peaks in fraction 32 derived from the final analytical RP-C4 chromatography. This indicated the existence of two fragments that could not be separated by chromatographic procedures. From ESI−MS, the exact molecular masses of both fragments were calculated to be 20 688 ± 2 and 20 428 ± 5 Da, respectively (parts A and B of Figure 2). Subsequently, the N-terminal sequence of both fragments was determined by Edman degradation and revealed the identical sequence GASPEQVADNGDDHSEGGLVENHVDST starting at Gly104 (Figure 2C). To determine the C-terminal amino acid residue of each fragment, the ESI−MS masses were compared to the calculated masses obtained from the pure IGFBP-2 amino acid sequence. The analysis showed that the two isolated fragments could be assigned to the amino acid residues 104−289 and 104−287 of IGFBP-2, respectively. The mass difference between the two fragments of 260 Da matched exactly the amino acids MQ absent in the shorter fragment IGFBP-2 (104−287) (Figure 2C).

Following this systematic approach, a total of 18 different IGFBP-2 fragments was identified and purified from the HF pH-pool eluates 5 and 6 (*15*). An overview of all identified fragments is shown in Table 1. Most fragments that were identified spanned the complete C-terminal region. The two fragments starting at Gly104 comprised the C-terminal domain and, in addition, the midregion of IGFBP-2. The N-terminal amino acid residues of other isolated fragments were determined to be Ala153, Glu157, Val159, Met166, Gly167, or Gly169, indicating cleavage after Leu152, Arg156, Lys158, Gln165, Met166, or Lys168, respectively (Table 1). The most prominent fragment identified was IGFBP-2 (167−279) occurring in a calculated concentration of >1 nM (>10 μg/L) in HF. Another fragment, IGFBP-2 (167−204 and 205−279), comprised exactly the same amino

Table 1: Identification of IGFBP-2 Fragments Isolated from Human HF

	N-terminal sequence analysis	molecular mass (Da)	amino acid residues
1	GASPEQVADNGDDHSEGGLV	20 684.5	104−289
2	GASPEQVADNGDDHSEGGLV	20 425.2	104−287
3	AVFREX[a]VTEQHRQMGKGGKH	15 764.1	153−289
4	EKVTEQHRQMGKGG	15 290.5	157−289
5	EKVTEQHRQMGKGG	15 031.2	157−287
6	VTEQHRQMGKGGKH	15 033.2	159−289
7	VTEQHRQMGKGGKH	14 773.9	159−287
8	MGKGX[a]KHHLGLEEPKKL	14 154.3	166−289
9	MGKGX[a]KHHLGLEEPKKL	13 895.0	166−287
10	GKX[a]GKHHLGLEEPKKLR	14 023.1	167−289
11	GKX[a]GKHHLGLEEPKKLR	13 885.0	167−288
12	GKX[a]GKHHLGLEEPKKLR	13 763.8	167−287
13[b]	GKGGKHHLGLEEPKK	12 857.7	167−279
14	GKGGKHHLGLEEPK	12 875.7	167−204
	MRLPDERGPLEHLY		205−279
15	GGKHHLGLEEPKKLRPP	13 584.5	169−287
16	GKGGKHHLGLEEPKKLX[a]PPPA	4244.9	167−204
17	MRLPDERGPLEHLYSL	9798.2	205−289
18	MRLPDERGPLEHLYSL	9538.9	205−287

[a] Some weak amino acid signals could not be assigned (X). [b] The most prominent fragment.

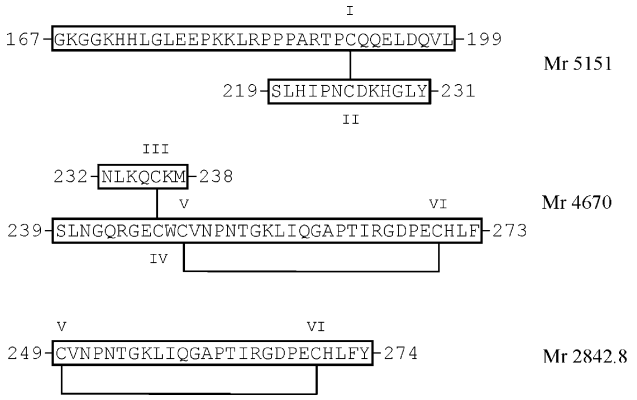

FIGURE 3: Disulfide bonding pattern of the C-terminal domain of IGFBP-2. To examine the disulfide bonding pattern of the C-terminal domain, the purified most abundant fragment IGFBP-2 (167−279) was digested with chymotrypsin and the resulting fragments were subsequently analyzed by MALDI−MS, ESI−MS, and N-terminal sequencing. Sequence analysis of two fragments with molecular masses of 5151 and 4670 Da (calculated molecular masses of 5153 and 4672 Da, respectively) resulted in characteristic double sequences demonstrating disulfide bonds between Cys191 and Cys225 and between Cys236 and Cys247, respectively. A third fragment with a molecular mass of 2842.8 Da comprising amino acid residues 249−274 (calculated molecular mass of 2842.4 Da) was analyzed indicating a disulfide bond between Cys249 and Cys270.

acid sequence but contained one internal hydrolyzed peptide bond between Thr204 and Met205 leading to an increase of the molecular mass of 18 Da (12 875 Da versus 12 858 Da; see Table 1, IGFBP2 fragments 14 and 13, respectively). The C-terminal end of the majority of the identified fragments corresponded to either the C terminus of IGFBP-2 (Gln289) or showed cleavage after Arg287, respectively. Additionally, three other proteolyzed fragments comprising only partial sequences of the C-terminal IGFBP-2 region, amino acid residues 167−204, 205−289, and 205−287, were detected (Table 1).

Disulfide Bonding Pattern of the C-Terminal IGFBP-2 Domain. Milligram amounts of the predominant fragment IGFBP-2 (167−279) were isolated from 10 000 L of human HF and purified to homogeneity. To determine the disulfide bonding pattern of the C-terminal IGFBP-2 domain, the peptide was proteolytically cleaved by the endoproteinase chymotrypsin. The obtained peptide fragments were subsequently analyzed by MALDI−MS, ESI−MS, and sequence analysis (Figure 3). The analyzed fragments with determined molecular masses of 5151 and 4670 Da showed characteristic double sequences that could be assigned to a disulfide bond between cysteines 191 and 225 as well as between cysteines 236 and 247 of IGFBP-2. The fragment with a molecular mass of 2842.8 Da showed a single sequence with characteristic signals for cysteine residues at positions 249 and 270, indicating the occurrence of another disulfide bridge between these two cysteine residues. Furthermore, the determined molecular mass of 2842.8 Da was exactly in accordance with the expected molecular mass of 2842.4 Da for the oxidized peptide (amino acid residues 249−274) confirming the disulfide bond between cysteine 249 and cysteine 270 of IGFBP-2.

IGF-Binding Properties of the Isolated IGFBP-2 Fragments. The five most prominent fragments that could be purified in sufficient amounts from HF were selected for analysis of their IGF-binding capacity in comparison to rhIGFBP-2. First, the fragments IGFBP-2 (104−289), IGFBP-2 (167−279), IGFBP-2 (157−289), and IGFBP-2 (167−289) and the fragment IGFBP-2 (167−204 and 205−279) containing one internal hydrolyzed peptide bond were separated by SDS−PAGE and examined by ligand blotting using either [^{125}I]IGF-I (Figure 4A) or biotinylated IGF-II (Figure 4B). The presence of the IGFBP-2 fragments was demonstrated by IGFBP-2 Western blotting (Figure 4C). Only the hydrolyzed fragment IGFBP-2 (167−204 and 205−279) showed a significant IGF-I-binding capability (Figure 4A). In contrast, the highest IGF-II-binding capability was observed for IGFBP-2 (167−279), whereas the hydrolyzed fragment IGFBP-2 (167−204 and 205−279) as well as the fragments IGFBP-2 (104−289) and IGFBP-2 (157−289) revealed only a low IGF-II-binding capability (Figure 4B). The fragment IGFBP-2 (167−289) failed to bind both IGF-I and IGF-II when analyzed by ligand blotting. To determine the IGF-I-binding properties more precisely, the affinity constants of IGFBP-2 (167−279) and the hydrolyzed fragment IGFBP-2 (167−204 and 205−279) were determined by equilibrium saturation studies incubating increasing amounts of the fragments or intact rhIGFBP-2 with [^{125}I]-IGF-I in solution (Figure 4D). The fragment IGFBP-2 (167−279) showed a ca. 150-fold reduced IGF-I affinity (K_d = 495 nM) compared to intact rhIGFBP-2 (K_d = 3.4 nM). Interestingly, the hydrolyzed fragment IGFBP-2 (167−204 and 205−279) showed only a ca. 35-fold reduced IGF-I affinity (K_d = 120 nM) compared to the intact rhIGFBP-2. In a third approach, the on-rate constant (k_a) and the off-rate constant (k_d) as well as the equilibrium rate constant (K_d) for the interaction of the selected fragments, intact rhIGFBP-2, and IGF-II were determined by SPR spectroscopy. IGF-II was immobilized on a sensor chip surface, followed by binding analysis of IGFBP-2 fragments in the analyte solution. The determined binding data are summarized in Figure 4E. The predominant fragment IGFBP-2 (167−279) showed an approximately 10-fold lower affinity for IGF-II (K_d = 43 nM) than intact IGFBP-2 (K_d = 4.1

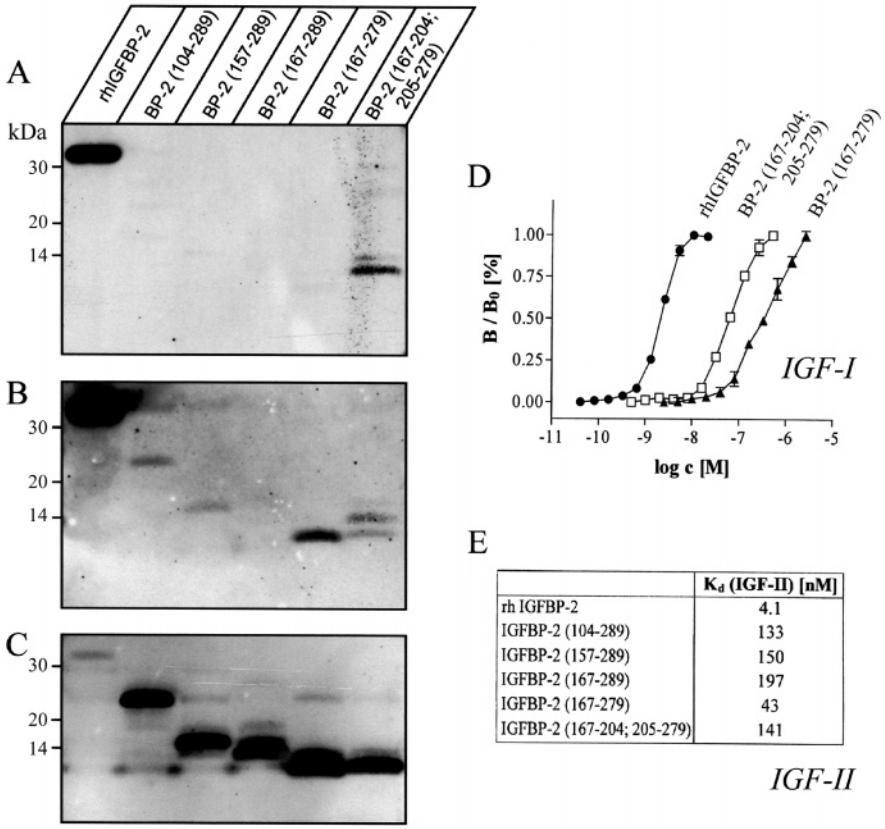

FIGURE 4: Binding of IGF-I and IGF-II to purified IGFBP-2 fragments. Intact rhIGFBP-2 (100 ng in A and B and 50 ng in C) and purified IGFBP-2 fragments (200 ng each) were separated by SDS−PAGE and analyzed in parallel by (A) IGF-I and (B) IGF-II ligand blotting as well as (C) IGFBP-2 immunoblotting. The positions of the molecular mass markers are indicated. The experiments were repeated 3 times with similar results. (D) Saturation binding assays using [^{125}I]IGF-I confirmed the reduced binding affinity of IGF-I to the hydrolyzed fragment IGFBP-2 (167−204 and 205−279) (□) and a very low affinity to the corresponding non-hydrolyzed fragment IGFBP-2 (167−279) (▲) compared to rhIGFBP-2 (●). The binding data represent the summary of two different experiments performed in triplicates. (E) BIAcore real-time measurements were carried out by passing rhIGFBP-2 and the indicated fragments over IGF-II-coated chip surfaces. The equilibrium rate constant K_d was calculated as described in the Material and Methods.

nM). The affinities of all other fragments were at least 30-fold lower compared to that of intact rhIGFBP-2.

DISCUSSION

The present study reports on the purification and characterization of 18 fragments of human IGFBP-2 generated *in vivo*. The molecular masses of the fragments comprising 37−185 amino acid residues vary between 4245 Da [IGFBP-2 (167−204)] and 20 685 Da [IGFBP-2 (104−289)]. The N-terminal sequences of most IGFBP-2 fragments start in the midregion and extend either to the C-terminal Gln289 residue or to the Arg287 residue of the hIGFBP-2 sequence (Figure 5). Several studies reporting on the proteolysis of IGFBP-2 *in vitro* or of naturally occurring IGFBP-2 fragments have demonstrated the formation of 2−3 fragments with apparent molar masses of 23−24 and 12−16 kDa estimated by SDS−PAGE (*13*, *22*, *30*−*34*). Purification and MS of a 24-kDa IGFBP-2 fragment from human milk resulted in the identification of N-terminal sequences starting with either residues Glu1 or Phe4 of IGFBP-2 (*13*). In comparison to the 31-kDa intact IGFBP-2, the data indicate that the 24-kDa IGFBP-2 fragment is C-terminally truncated. The analysis of two other 14−16-kDa IGFBP-2 fragments in milk showed amino-terminal sequences starting at Gly169 and Lys181 with predicted molecular masses of 13 786 and 12 502 Da, respectively (*13*). Wang et al. (*11*) have identified

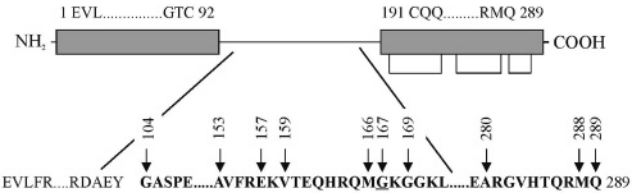

FIGURE 5: Structure and proteolytic cleavage sites of human IGFBP-2 as determined in human HF are schematically demonstrated. The cysteine-rich N- and C-terminal domains are indicated by gray boxes. The various proteolytic cleavage sites in the variable midregion and the C-terminal domain with the exception of the cleavage site between Thr204 and Met205 are marked by arrows. The disulfide bond pattern in the conserved C-terminal domain is indicated below the diagram.

a 14-kDa IGFBP-2 fragment in conditioned media of the rat liver BRL-3A cell line starting at Met148, which corresponds to Met166 of human IGFBP-2. Corresponding fragments were also found in the human HF peptide library [Table 1, peptide 8, IGFBP-2 (166−289) and peptide 15, IGFBP-2 (169−287)]. The great diversity of IGFBP-2 fragments occurring in the circulation and described in this study was surprising. It is tempting to speculate that the great variety of IGFBP-2 fragments could be due to different proteolytic activities within different tissues. It is proposed that binary IGF−IGFBP-2 complexes can leave the circulation and localize to specific tissues. After the binding to

different cell types, cleavage could occur at the cell membrane to deliver the IGF to their cell-surface receptors. As the renal filtration is reduced in the HF patients, all of these fragments would concentrate in the blood and could finally be detected.

However, at least in the circulating IGFBP-2, the presented data indicate 4 major cleavage sites between Tyr103 and Gly104, Leu152 and Ala153, Arg156 and Glu157, and Gln165 and Met166 and further modification of the resulting fragments by amino and/or carboxy peptidases (mono-, di-, and tripeptidases). Furthermore, a cleavage site was identified in the conserved C-terminal domain between Thr204 and Met205 generating a hydrolyzed fragment 14 [Table 1, IGFBP-2 (167−204 and 205−279)], which is obviously stabilized by disulfide bridges, as well as three smaller IGFBP-2 fragments comprising the residues 167−204, 205−289, and 205−287 (Table 1, peptides 16−18).

Elevated serum levels of IGFBP fragments have been reported during pregnancy and under catabolic and disease status (*30*, *35*−*38*) caused by increased IGFBP protease activities and reduced glomerular clearance (*20*, *39*, *40*). The absence of detectable IGFBP-2 protease activity in the serum of patients with chronic renal failure (CRF) (B. Kübler, unpublished results), as well as the lack of protease activities cleaving IGFBP-3 (*29*, *41*, *42*) or IGFBP-4 (*28*), suggests that the increased amounts of IGFBP fragments may be the result either of reduced renal filtration of the cleavage products generated by basal IGFBP proteases or of proteases in other tissues. Proteolyzed IGFBP-2 fragments have been detected in serum (*43*), HF (*15*), follicular fluid (*30*, *31*), cerebrospinal fluid (*44*), and milk (*13*). The origin of the protease responsible for the generation of IGFBP-2 fragments in milk is also a matter of debate proposing either the cleavage of IGFBP-2 before secretion from the mammary gland (*13*) or the presence of high IGFBP-2 protease activity in the milk (*45*). On the basis of inhibitor studies, the latter has been classified as cation-dependent kallikrein-like serine protease (*45*). Whereas the IGFBP-2 protease in uterine flushings of pregnant gilts was also inhibited by specific kallikrein inhibitors (*34*), the IGFBP-2 protease in bovine and porcine preovulatory follicular fluids has been identified as pregnancy-associated plasma protein-A (PAPP-A) cleaving IGFBP-2 between Gln165 and Met166 *in vitro* (*31*). This cleavage could be confirmed by our findings (Figure 5), suggesting PAPP-A as one important IGFBP-2 protease in the plasma of patients suffering from CRF. Further major cleavages may be caused by trypsin-like (e.g., plasmin) and chymotrypsin-like proteases.

Several studies have shown that both the amino- and carboxy-terminal conserved domains of IGFBP-2 bind IGFs. Thus, iodination protection experiments suggest the involvement of Tyr60 in the IGF-binding site (*46*), and BIAcore analysis with recombinant amino-terminal IGFBP-2 fragments (1−132 and 1−185) has demonstrated the capability for rapid association with IGFs (*14*). Also naturally occurring carboxy-terminal IGFBP-2 fragments [amino acid residues 148−270 of rat IGFBP-2 (*11*) and 169−289 of human IGFBP-2 (*13*)] or recombinant carboxy-terminal fragments of bovine IGFBP-2 have been shown to retain IGF-binding capacity and appear to maintain IGF in a complexed form (*14*). Furthermore, photoaffinity labeling experiments with human IGFBP-2 and analyses of C-terminally truncated IGFBP-2 have indicated that the IGF-binding sites comprise the amino acid residues 212−227 and 266−287 of human IGFBP-2 and 222−236 of bovine IGFBP-2, respectively (*12*, *47*). The present study has confirmed the IGF-binding ability of five carboxy-terminal IGFBP-2 fragments purified from human HF in sufficient amounts. Ligand blot analysis revealed that IGFBP-2 fragments 104−289, 157−289, and 167−279 and the hydrolyzed fragments 167−204 and 205−279 retained IGF-II-binding capacity. Further analysis in BIAcore real-time measurements showed that the most prominent fragment IGFBP-2 (167−279) revealed the strongest binding affinity to IGF-II, which was estimated to be 10-fold lower than that of intact IGFBP-2. Surprisingly, IGF-I only weakly interacted with this fragment but instead bound 4-fold better to the corresponding IGFBP-2 fragment with the hydrolyzed peptide bond between Thr204 and Met205 when measured by the saturation binding assay in solution. This was also in accordance with the observation that the hydrolyzed fragment showed a higher binding to IGF-I in IGF-I ligand blotting than the nonhydrolyzed fragment. In contrast, the affinity of the hydrolyzed fragment for IGF-II was 3-fold reduced compared to the nonhydrolyzed fragment. These data suggest that a lower structural flexibility in the C-terminal region of the intact IGFBP-2 might contribute to the difference in relative affinity of IGFBP-2 for IGF-II over IGF-I (*48*).

In contrast to IGFBP-3 (*29*) or IGFBP-4 (*28*), in the present study, no amino-terminal IGFBP-2 fragments starting at Glu1 could be detected. The used polyclonal antiserum sensitively recognized N-terminal IGFBP-2 fragments, and therefore we exclude the occurrence of such fragments in detectable amounts in human HF. This suggests either a specific mechanism for the removal of IGFBP-2 fragments containing the N-terminal domain or the inclusion of these fragments in higher molecular mass complexes preventing the appearance in the HF.

Analysis of the disulfide bond pattern in the C-terminal domain of human IGFBP-2 revealed disulfide bridges between Cys191 and Cys225, Cys236 and Cys247, and Cys249 and Cys270, confirming the pattern found in the bovine IGFBP-2 (*12*). This C-terminal disulfide pattern seems to present a consensus pattern for all IGFBPs (*28*, *49*).

Our finding of diverse C-terminal IGFBP-2 fragments revealing a reduced IGF affinity and comprising the integrin-binding motif RGD (residues 265−267), which might allow the binding to the $\alpha_5\beta_1$ integrin (*50*), as well as the proteoglycan-binding domain, confirms the assumption that after celluar binding and proteolysis of IGFBP-2 the IGFs may be released in close vicinity of IGF receptors. In this context, the C-terminal IGFBP-2 domain may direct and accelerate IGF binding to their receptors. The potential functional role of C-terminal IGFBP-2 fragments in different cellular and tissue compartments of the body remains to be examined.

ACKNOWLEDGMENT

The authors thank Ute Block and Tobias Marquardt for their excellent experimental support. We gratefully thank Dr. Andreas Höflich for providing a vector for expression of rhIGFBP-2 (1−147).

REFERENCES

1. Rechler, M. M., and Brown, A. L. (1992) Insulin-like growth factor binding proteins: Gene structure and expression, *Growth Regul. 2*, 55−68.
2. Zapf, J. (1995) Physiological role of the insulin-like growth factor binding proteins, *Eur. J. Endocrinol. 132*, 645−654.
3. Jones, J. I., and Clemmons, D. R. (1995) Insulin-like growth factors and their binding proteins: Biological actions, *Endocr. Rev. 16*, 33−34.
4. Lalou, C., Lassarre, C., and Binoux, M. (1996) A proteolytic fragment of insulin-like growth factor (IGF) binding protein-3 that fails to bind IGFs inhibits the mitogenic effects of IGF-I and insulin, *Endocrinology 137*, 3206−3212.
5. Oh, Y., and Rosenfeld, R. G. (1999) IGF-independent actions of the IGF binding proteins, in *The IGF System* (Rosenfeld, R. G., and Roberts, C. T., Jr., Eds.) pp 257−272, Humana Press Inc., Totowa, NJ.
6. Firth, S. M., and Baxter, R. C. (2002) Cellular actions of the insulin-like growth factor binding proteins, *Endocr. Rev. 23*, 824−854.
7. Bunn, R. C., and Fowlkes, J. L. (2003) Insulin-like growth factor binding protein proteolysis, *Trends Endocrinol. Metab. 14*, 176−181.
8. Singh, B. K., Charkowicz, D. A., and Mascarenhas, D. D. (2004) IGF-independent effects mediated by a C-terminal metal-binding domain of insulin-like growth factor binding protein-3, *J. Biol. Chem. 279*, 477−487.
9. Baxter, R. C. (2000) Insulin-like growth factor (IGF)-binding proteins: Interactions with IGFs and intrinsic bioactivities, *Am. J. Physiol. Endocrinology Metab. 278*, E967−E976.
10. Roghani, M., Lassarre, C., Zapf, J., Povoa, G., and Binoux, M. (1991) Two insulin-like growth factor (IGF)-binding proteins are responsible for the selective affinity for IGF-II of cerebrospinal fluid binding proteins, *J. Clin. Endocrinol. Metab. 73*, 658−666.
11. Wang, J. F., Hampton, B., Mehlman, T., Burgess, W. H., and Rechler, M. M. (1988) Isolation of a biologically active fragment from the carboxy terminus of the fetal rat binding protein for insulin-like growth factors, *Biochem. Biophys. Res. Commun. 157*, 718−726.
12. Forbes, B. E., Turner, D., Hodge, S. J., McNeil, K. A., Forsberg, G., and Wallace, J. C. (1998) Localization of an insulin-like growth factor (IGF) binding site of bovine IGF binding protein-2 using disulfide mapping and deletion mutation analysis of the C-terminal domain, *J. Biol. Chem. 273*, 4647−4652.
13. Ho, P. J., and Baxter, R. C. (1997) Characterization of truncated insulin-like growth factor-binding protein-2 in human milk, *Endocrinology 138*, 3811−3818.
14. Carrick, F. E., Forbes, B. E., and Wallace, J. C. (2001) BIAcore analysis of bovine insulin-like growth factor (IGF)-binding protein-2 identifies major IGF binding site determinants in both the amino- and carboxyl-terminal domains, *J. Biol. Chem. 276*, 27120−27128.
15. Ständker, L., Kübler, B., Obendorf, M., Braulke, T., Forssmann, W. G., and Mark, S. (2003) *In vivo* processed fragments of IGF binding protein-2 copurified with bioactive IGF-II, *Biochem. Biophys. Res. Commun. 304*, 708−713.
16. Conover, C. A., and Khosla, S. (2003) Role of extracellular matrix in insulin-like growth factor (IGF) binding protein-2 regulation of IGF-II action in normal human osteoblasts, *Growth Horm. IGF Res. 13*, 328−335.
17. Russo, V. C., Bach, L. A., Fosang, A. J., Baker, N. L., Werther, G. A. (1997) Insulin-like growth factor binding protein-2 binds to cell surface proteoglycans in the rat brain olfactory bulb, *Endocrinology 138*, 4858−4867.
18. Fowlkes, J. L., Serra, D. M., Bunn, R. C., Thrailkill, K. M., Enghild, J. J., and Nagase, H. (2004) Regulation of insulin-like growth factor (IGF)-I action by matrix metalloproteinase-3 involves selective disruption of IGF-I/IGF-binding protein-3 complexes, *Endocrinology 145*, 620−626.
19. Shalamanova, L., Kübler, B., Scharf, J. G., and Braulke, T. (2001) MDCK cells secrete neutral proteases cleaving insulin-like growth factor-binding protein-2 to -6, *Am. J. Physiol. Endocrinol. Metab. 281*, E1221−E1229.
20. Maile, L. A., and Holly, J. M. (1999) Insulin-like growth factor binding protein (IGFBP) proteolysis: Occurrence, identification, role, and regulation, *Growth Horm. IGF Res. 9*, 85−95.
21. Shi, Z., Xu W., Loechel, F., Wewer, U. M., and Murphy, L. J. (2000) ADAM 12, a disintegrin metalloprotease, interacts with insulin-like growth factor-binding protein-3, *J. Biol. Chem. 275*, 18574−18580.
22. Claussen, M., Kübler, B., Wendland, M., Neifer, K., Schmidt, B., Zapf, J., and Braulke, T. (1997) Proteolysis of insulin-like growth factors (IGF) and IGF binding proteins by cathepsin D, *Endocrinology 138*, 3797−3803.
23. Moralez, A., Busby, W. H., Jr., and Clemmons, D. (2003) Control of insulin-like growth factor binding protein-5 protease synthesis and secretion by human fibroblasts and porcine aortic smooth muscle cells, *Endocrinology 144*, 2489−2495.
24. Booth, B. A., Boes, M., and Bar, R. S. (1996) IGFBP-3 proteolysis by plasmin, thrombin, serum: Heparin binding, IGF binding, and structure of fragments, *Am. J. Physiol. 271*, E465−E470.
25. Schulz-Knappe, P., Schrader, M., Ständker, L., Richter, R., Hess, R., Jürgens, M., and Forssmann, W. G. (1997) Peptide bank generated by large-scale preparation of circulating human peptides, *J. Chromatogr., A 776*, 125−132.
26. Mark, S., Forssmann, W. G., and Ständker, L. (1999) Strategy for identifying circulating fragments of insulin-like growth factor binding proteins in a hemofiltrate peptide bank, *J. Chromatogr., A 852*, 197−205.
27. Hossenlopp, P., Seurin, D., Segovia-Quinson, B., Hardouin, S., and Binoux, M. (1986) Analysis of serum insulin-like growth factor binding proteins using western blotting: Use of the method for titration of the binding proteins and competitive binding studies, *Anal. Biochem. 154*, 138−143.
28. Ständker, L., Braulke, T., Mark, S., Mostafavi, H., Meyer, M., Höning, S., Gimenez-Gallego, G., and Forssmann, W. G. (2000) Partial IGF affinity of circulating N- and C-terminal fragments of human insulin-like growth factor binding protein-4 (IGFBP-4) and the disulfide bonding pattern of the C-terminal IGFBP-4 domain, *Biochemistry 39*, 5082−5088.
29. Kübler, B., Draeger, C., John, H., Andag, U., Scharf, J. G., Forssmann, W. G., Braulke, T., and Ständker, L. (2002) Isolation and characterization of circulating fragments of the insulin-like growth factor binding protein-3, *FEBS Lett. 518*, 124−128.
30. Giudice, L. C., Farrell, E. M., Pham, H., and Rosenfeld, R. G. (1990) Identification of insulin-like growth factor-binding protein-3 (IGFBP-3) and IGFBP-2 in human follicular fluid, *J. Clin. Endocrinol. Metab. 71*, 1330−1338.
31. Monget, P., Mazerbourg, S., Delpuech, T., Maurel, M. C., Maniere, S., Zapf, J., Lalmanach, G., Oxvig, C., and Overgaard, M. T. (2003) Pregnancy-associated plasma protein-A is involved in insulin-like growth factor binding protein-2 (IGFBP-2) proteolytic degradation in bovine and porcine preovulatory follicles: Identification of cleavage site and characterization of IGFBP-2 degradation, *Biol. Reprod. 68*, 77−86.
32. Cohick, W. S., Gockerman, A., and Clemmons, D. R. (1993) Vascular smooth muscle cells synthesize two forms of insulin-like growth factor binding proteins which are regulated differently by the insulin-like growth factors, *J. Cell. Physiol. 157*, 52−60.
33. Elmlinger, M. W., Rauschnabel U., Koscielniak, E., Weber, K., Ranke, M. B. (1999) Secretion of noncomplexed 'Big' (10−18 kD) forms of insulin-like growth factor-II by 12 soft tissue sarcoma cell lines, *Horm. Res. 52*, 178−185.
34. Geisert, R. D., Chamberlain, C. S., Vonnahme, K. A., Malayer, J. R., and Spicer, L. J. (2001) Possible role of kallikrein in proteolysis of insulin-like growth factor binding proteins during the oestrous cycle and early pregnancy in pigs, *Reproduction 121*, 719−728.
35. Hossenlopp, P., Segovia, B., Lassarre, C., Roghani, M., Bredon, M, and Binoux, M. (1990) Evidence of enzymatic degradation of insulin-like growth factor-binding proteins in the 150K complex during pregnancy, *J. Clin. Endocrinol. Metab. 71*, 797−805.
36. Bereket, A., Lang, C. H., Blethen, S. L., Fan, J., Frost, R. A., and Wilson, T. A. (1995) Insulin-like growth factor binding protein-3 proteolysis in children with insulin-dependent diabetes mellitus: A possible role for insulin in the regulation of IGFBP-3 protease activity, *J. Clin. Endocrinol. Metab. 80*, 2282−2288.
37. Whellams, E. J., Maile, L. A., Fernihough, J. K., Billingham, M. E., and Holly, J. M. (2000) Alterations in insulin-like growth factor binding protein-3 proteolysis and complex formation in the arthritic joint. *J. Endocrinol. 165*, 545−556.
38. Tönshoff, B., Blum, W. F., Wingen, A. M., and Mehls, O. (1995) Serum insulin-like growth factors (IGFs) and IGF binding proteins 1, 2, and 3 in children with chronic renal failure: Relationship to height and glomerular filtration rate. The European Study Group for Nutritional Treatment of Chronic Renal Failure in Childhood. *J. Clin. Endocrinol. Metab. 80*, 2684−2691.

39. Byun, D., Mohan, S., Yoo, M., Sexton, C., Baylink, D. J., and Qin, X. (2001) Pregnancy-associated plasma protein-A accounts for the insulin-like growth factor (IGF)-binding protein-4 (IGFBP-4) proteolytic activity in human pregnancy serum and enhances the mitogenic activity of IGF by degrading IGFBP-4 *in vitro*, *J. Clin. Endocrinol. Metab. 86*, 847−854.
40. Tönshoff, B., Schaefer, F., and Mehls, O. (1990) Disturbance of growth hormone−insulin-like growth factor axis in uraemia. Implications for recombinant human growth hormone treatment, *Pediatr. Nephrol. 4*, 654−662.
41. Lee, K. O., Oh, Y., Giudice, L. C., Cohen, P., Peehl, D. M., and Rosenfeld, R. G. (1994) Identification of insulin-like growth factor-binding protein-3 (IGFBP-3) fragments and IGFBP-5 proteolytic activity in human seminal plasma: A comparison of normal and vasectomized patients, *J. Clin. Endocrinol. Metab. 79*, 1367−1372.
42. Powell, D. R., Durham, S. K., Liu, F., Baker, B. K., Lee, P. D., Watkins, S. L., Campbell, P. G., Brewer, E. D., Hintz, R. L., and Hogg, R. J. (1998) The insulin-like growth factor axis and growth in children with chronic renal failure: A report of the Southwest Pediatric Nephrology Study Group, *J. Clin. Endocrinol. Metab. 83*, 1654−1661.
43. McCusker, R. H., Cohick, W. S., Busby, W. H., and Clemmons, D. R. (1991) Evaluation of the developmental and nutritional changes in porcine insulin-like growth factor-binding protein-1 and -2 serum levels by immunoassay, *Endocrinology 129*, 2631−2638.
44. Roghani, M., Hossenlopp, P., Lepage, P., Balland, A., and Binoux, M. (1989) Isolation from human cerebrospinal fluid of a new insulin-like growth factor-binding protein with a selective affinity for IGF-II, *FEBS Lett. 255*, 253−258.
45. Elmlinger, M. W., Grund, R., Buck, M., Wollmann, H. A., Feist, N., Weber, M. M., Speer, C. P., and Ranke, M. B. (1999) Limited proteolysis of the IGF binding protein-2 (IGFBP-2) by a specific serine protease activity in early breast milk, *Pediatr. Res. 46*, 76−81.
46. Hobba, G. D., Forbes, B. E., Parkinson, E. J., Francis, G. L., and Wallace, J. C. (1996) The insulin-like growth factor (IGF) binding site of bovine insulin-like growth factor binding protein-2 (bIGFBP-2) probed by iodination, *J. Biol. Chem. 271*, 30529−30536.
47. Horney, M. J., Evangelista, C. A., and Rosenzweig, S. A. (2001) Synthesis and characterization of insulin-like growth factor (IGF)-1 photoprobes selective for the IGF-binding proteins (IGFBPS). photoaffinity labeling of the IGF-binding domain on IGFBP-2, *J. Biol. Chem. 276*, 2880−2889.
48. Szabo, L., Mottershead, D. G., Ballard, F. J., and Wallace, J. C. (1988) The bovine insulin-like growth factor (IGF) binding protein purified from conditioned medium requires the N-terminal tripeptide in IGF-1 for binding, *Biochem. Biophys. Res. Commun. 151*, 207−214.
49. Chelius, D., Baldwin, M. A., Lu, X,. and Spencer, E. M. (2001) Expression, purification, and characterization of the structure and disulfide linkages of insulin-like growth factor binding protein-4, *J. Endocrinol. 168*, 283−296.
50. Schütt, B. S., Langkamp, M., Rauschnabel, U., Ranke, M. B., and Elmlinger, M. W. (2004) Integrin-mediated action of insulin-like growth factor binding protein-2 in tumor cells, *J. Mol. Endocrinol. 32*, 859−868.

BI0478401